



Comparative Analysis of Measurement Points for Structural Damage Identification in Free-Free Aluminium Beam using Response Surface Methodology and FRF Curvature

Nur Raihana Sukri^{1,2}, Nurulakmar Abu Husain^{1,*}, Syarifah Zyurina Nordin¹, Aminudin Abu¹

¹ Malaysia-Japan International Institute of Technology, Universiti Teknologi Malaysia, 54100 Kuala Lumpur, W.P.Kuala Lumpur, Malaysia

² Jabatan Kejuruteraan Mekanikal, Politeknik Banting, 42700 Banting, Selangor, Malaysia

ARTICLE INFO

Article history:

Received 12 February 2024

Received in revised form 9 April 2024

Accepted 23 April 2024

Available online 30 May 2024

Keywords:

FRF curvature; response surface methodology; model updating; structural damage identification

ABSTRACT

This research paper presents a comprehensive comparative analysis of measurement points for structural damage identification in free-free aluminium beams using Response Surface Methodology (RSM) and Frequency Response Function (FRF) curvature. The primary objective is to determine the optimal measurement points for establishing a relationship between the input parameters and response features, thus forming a surrogate model. The investigation focuses on analyzing the influence of the number of measurement points on RSM's capability to identify structural damage. Three distinct Design of Experiment (DOE) techniques are explored: central composite design (CCD), Box-Behnken design (BBD), and D-optimal design, each incorporating different numbers of measurement points (10 elements, 15 elements, and 20 elements). The study's results highlight BBD's strong capability in detecting damage with fewer measurement points, while CCD design accurately identifies damage in finer measurement points. The findings reveal a clear trend: as the number of measurement points increases, the model becomes more refined, yielding higher stiffness reduction factor (SRF) values. The results underscore the significance of selecting an appropriate number of measurement points to enhance RSM's efficiency in identifying structural damage, thereby optimizing damage identification processes. This study contributes valuable insights into the selection of measurement points for effective structural damage identification, offering practical implications for engineering applications.

1. Introduction

The identification of structural damage play pivotal roles in ensuring the safety, longevity, and functionality of various engineering structures [1]. Conventional damage identification methods may overlook subtle damage shifts in Frequency Response Functions (FRF), but leveraging FRF curvature can amplify these differences, improving sensitivity [2]. The FRF curvature method, as developed by Sampaio, Maia [3] proves efficacious by comparing intact and damaged structures across all

* Corresponding author.

E-mail address: nurulakmar@utm.my

<https://doi.org/10.37934/aram.117.1.204212>

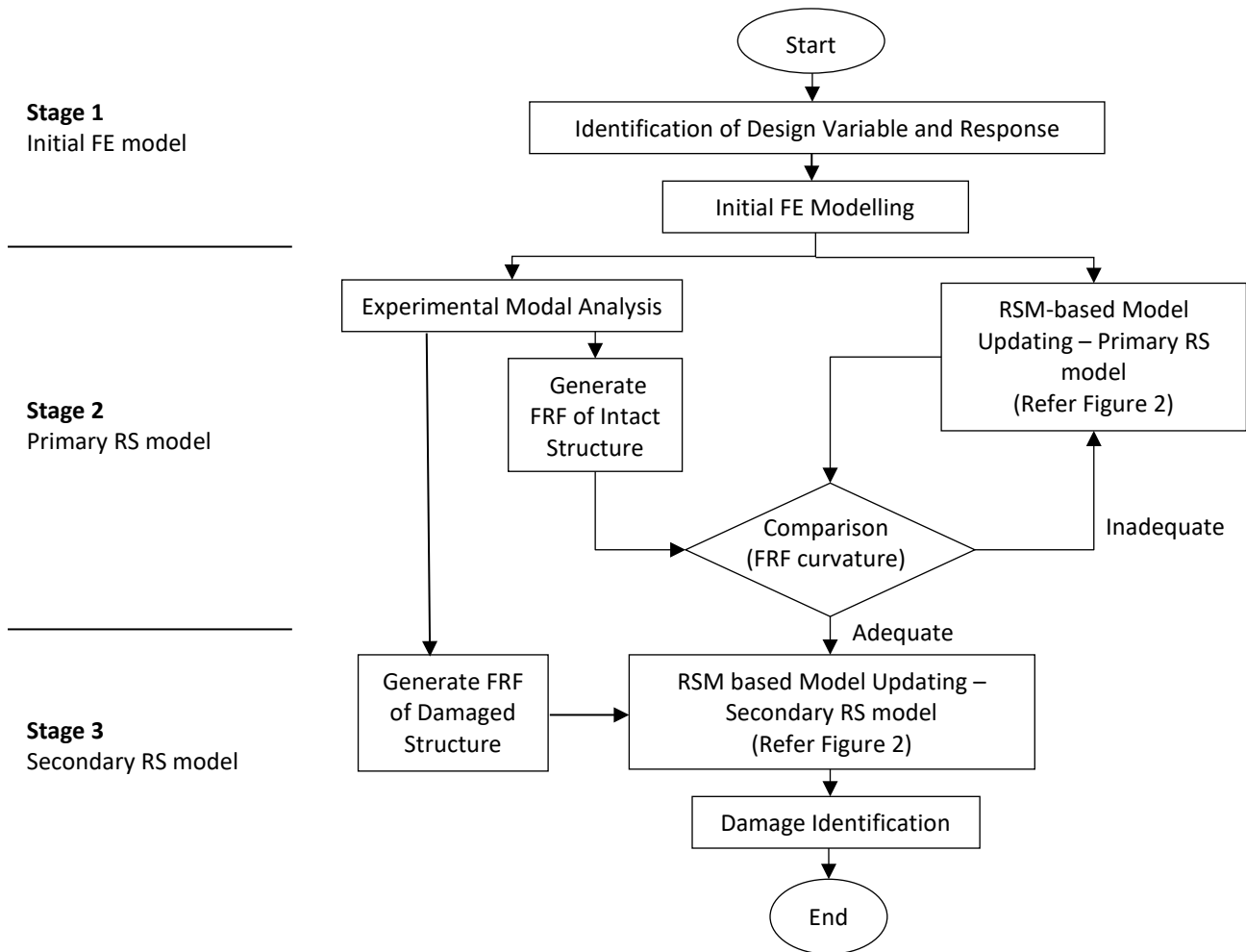
frequencies. Recognizing the need for more accurate and reliable results, recent studies on damage identification using FRF curvature method underscore the significance of increasing the number of measurement points or sensors [4]. In this context, the work of Porcu, Patteri [5] sheds light on the pivotal role of the distance between measurement points in optimizing the effectiveness of the FRF curvature approach. Employing a suitably fine mesh for measurement points has been shown to yield efficient and precise outcomes in structural damage identification.

In parallel, Response Surface Methodology (RSM) emerges as a tool to optimize engineering tasks, replacing complex calculations with surrogate model [6,7]. This surrogate model eliminates the need for complex calculations inherent in the full finite element model, thereby significantly enhancing computing efficiency and cost-effectiveness of the damage identification process. The current RSM-based damage identification method relies on natural frequencies and mode shapes as responses but faces challenges with false damage detection due to errors in modelling and response measurement. Consequently, the algorithm lacks reliability in accurately pinpointing damage [8]. Despite the lower measurement errors exhibited by the FRF compared to modal data, it has not been extensively employed as a response parameter in RSM-based damage identification due to its wide frequency range [9]. Therefore, this study integrates FRF curvature and RSM to enhance damage identification. This paper focuses on analyzing the influence of the number of measurement points on RSM's capability to identify structural damage. Three distinct Design of Experiment (DOE) techniques are explored: central composite design (CCD), Box-Behnken design (BBD), and D-optimal design, each incorporating different numbers of measurement points (10 elements, 15 elements, and 20 elements). The results aid in selecting measurement points for RSM-based model updating using FRF curvature as the response for damage identification. Ultimately, this research significantly contributes to the advancement of structural health monitoring and damage assessment techniques.

2. Methodology

The current RSM-based method for detecting structural damage, relying on natural frequencies and mode shapes, is unreliable due to errors [2]. Using FRF data is less error-prone but underused in RSM due to its wide range [10]. This study explores using FRF curvature as a response for better damage identification. The FRF curvature approach, by Sampaio and Maia [11], is promising but lacks research [12-15]. RSM establishes a relationship between design variables and responses [16-19]. The methodology for developing the RSM for damage identification using FRF curvature is illustrated in Figure 1 where it consists of three main stages.

Stage 1 encompasses the crucial step of selecting the key parameters that hold substantial influence over the model. These design variables can encompass a range of properties, including geometric attributes or material characteristics. For this research, Young's modulus is identified as the primary design variable, and the response is represented by the FRF curvature. Consequently, the initial finite element (FE) model is constructed using the initial Young's modulus value (E_i) as the basis for further analysis. Stage 2 involves constructing a primary response surface (RS) model by updating the FE model through RSM and assessing changes in FRF curvature for accuracy. The Young's modulus values for intact case (E'_i) are obtained through the model-updating process. In Stage 3, the focus shifts to damage identification. To detect damage, model updating is employed on the secondary RS model. Young's modulus values for damaged elements (E_d) are compared to intact values (E'_i) to calculate the stiffness reduction factor (SRF) as defined in Eq. (1), indicating damage severity [8].



$$SRF = 1 - \left(\frac{E_d}{E_i'} \right) \quad (1)$$

Fig. 1. RSM damage identification with FRF curvature as the response

The details of the process of RSM-based model updating using FRF curvature are illustrated in Figure 2. The DOE process involves selecting the updating design variables and setting the lower and upper bounds for their initial values. Four DOEs are compared: CCDmrv, CCDfrac, BBD, and D-Optimal. The FRF curvature response is computed using FE analysis based on the chosen DOE. The FRF curvature is determined at 96% of the first FRF resonance, following the recommendation outlined by Mondal, Mondal [20], and employing the equation proposed by Sampaio, Maia [3]. Eq. (2) defines the FRF curvature for any given frequency, with $H_{i,j}$ representing the receptance FRF measured at location i for a force input at location j .

$$H_{i,j}'' = \frac{H_{i+1,j} - 2H_{i,j} + H_{i-1,j}}{h^2} \quad (2)$$

Next, the quadratic RS model is constructed to establish the relationship between the response and design variables. The RS model's accuracy is evaluated using R-squared (R^2), adjusted R-squared (R^2_{adj}), and predicted R-squared (R^2_{pred}) as defined by Eq. (3), Eq. (4) and Eq. (5), respectively [21-23]. R^2 represents the amount of dispersion explained by the RS model around the mean [22]. However, the inclusion of insignificant parameter to the model increases the value of R^2 . As a result, the value of R^2_{adj} and R^2_{pred} must be verified. Their values should approach 1, with a marginal difference of 0.2

between them. Notably, the values of R^2_{adj} and R^2_{pred} decrease with the inclusion of insignificant parameters [17,22].

$$R^2 = \left(\frac{SS_R}{SS_T} \right) = 1 - \left(\frac{SS_E}{SS_T} \right), \quad 0 \leq R^2 \leq 1 \quad (3)$$

$$R^2_{adj} = 1 - \frac{SS_E/(n-p)}{SS_T/(n-1)} = 1 - \frac{n-1}{n-p} (1 - R^2) \quad (4)$$

$$R^2_{pred} = 1 - \frac{PRESS}{SS_T} \quad (5)$$

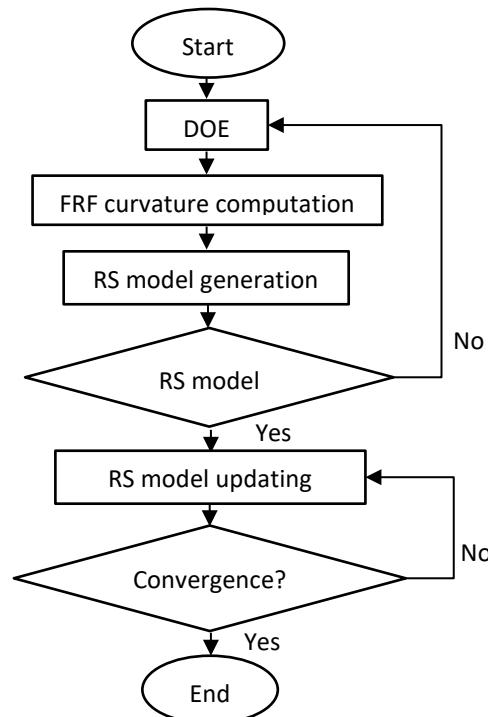


Fig. 2. RSM-based model updating

After the model is validated, it must be updated to minimize the discrepancy between the FRF curvature obtained from the RS model and the experimental data. A multi-objective optimization algorithm is formulated, as outlined in Eq. (6).

$$\min_{x,\gamma} \begin{cases} F(x) - \omega\gamma \leq goal \\ lb \leq x \leq ub \end{cases} \quad (6)$$

where $F(x)$ is the objective function, γ is a dummy variable, and ω is weight to control the attainment of the objectives, $goal$ is the desired value to achieve, lb is the lower bound, and ub is the upper bound. The objective function used in this study is defined in Eq. (7).

$$F(x) = abs \left(\frac{H''_{RSM} - H''_{exp}}{H''_{exp}} \right) \quad (7)$$

where H''_{RSM} and H''_{exp} represent the FRF curvature from the RSM and the experiment, respectively. MATLAB's multi-objective optimization algorithm *fgoalattain* is employed in the updating process. The optimization results provide the values of Young's modulus for each element.

3. Experimental Modal Analysis: Free-Free Aluminium Beam

To avoid boundary effects in experiments, free-free conditions were used for intact and damaged beams. Nylon fishing lines suspended the beams from a steel support frame to simulate free conditions accurately. Key properties were elastic modulus 71 GPa, density 2700 kg/m³, and Poisson's ratio 0.33. The aluminium beam was 1000 mm long with a cross-section of 0.25 m x 0.06 m. The beam was divided into sections: 10 elements, 15 elements and 20 elements as shown in Figure 3 (a). To test damage detection ability, 1 mm wide saw cuts were intentionally made at three places as visually depicted in Figure 3 (b). The cuts were 1 mm deep as presented in Figure 3 (c).

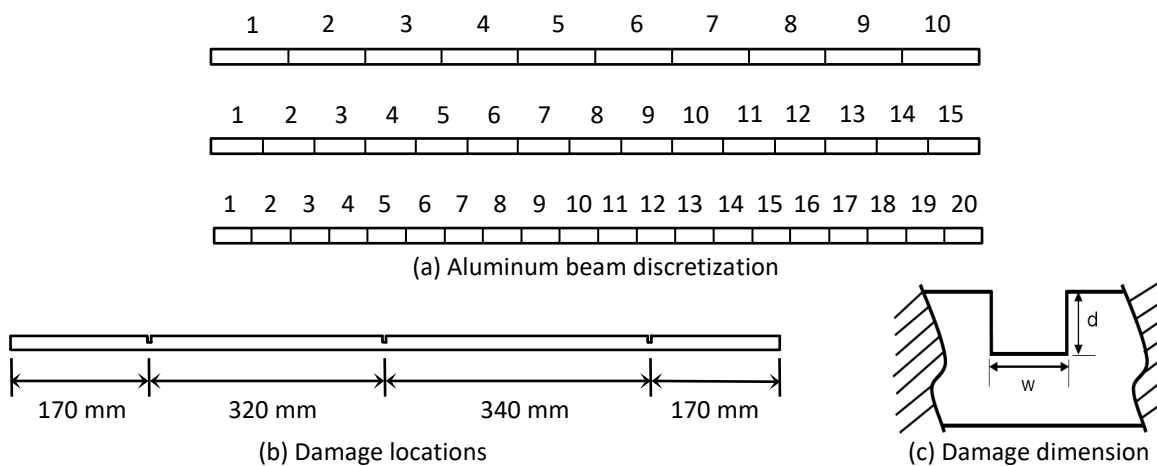


Fig. 3. Specimen setup

An experimental setup (Figure 4) included a Dytran Dytranpulse™ 5800B4 instrumented hammer with a sensitivity of 10.17 mV/lbf, a Dytran 3133A1 accelerometer having a sensitivity of 10.15493 mV/g and a mass of 0.8 g, along with an LMS SCADAS Mobile four-channel data acquisition unit and Simcenter Testlab software for the acquisition and analysis of signals. Responses were measured at each node using an accelerometer. Impact was applied at different nodes: node 6 for 10-element, node 9 for 15-element, and node 11 for 20-element beams, using an impact hammer.

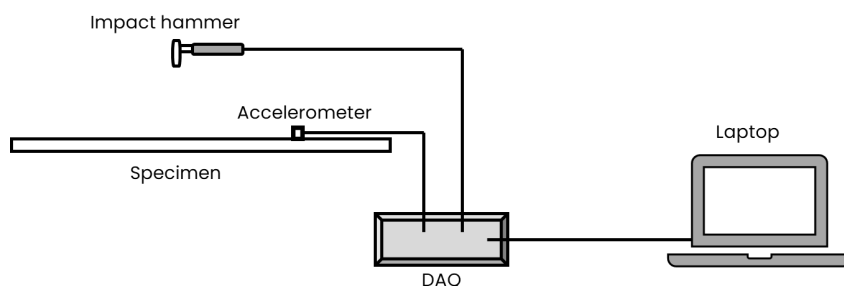


Fig. 4. Schematic diagram of impact hammer modal testing

4. Results

4.1 Impact of Measurement Points on DOE Performance

Structural damage severity is assessed through SRF, which reflects stiffness alterations. Higher values correspond to more severe damage. Figure 5 presents the calculated SRF values, with

highlighted elements indicating actual damage. With 10 elements, it captures basic structural behaviour, but intricate stiffness changes might not be fully captured. BBD stands out in damage identification, minimizing false damage locations and closely aligning with real positions.

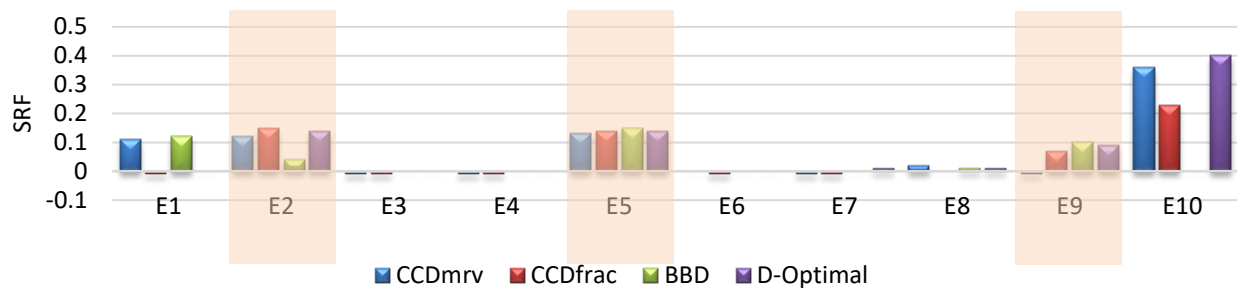


Fig. 5. SRF from CCDmrv, CCDhalf, BBD and D-Optimal for 10 elements

With 15 elements, the model is refined, capturing localized damage better. This results in a higher SRF around 0.20, indicating stiffness reduction from damage. Figure 6 illustrates D-Optimal excelling in damage detection, reducing incorrect damage locations and aligning well with actual damage areas. CCD and BBD designs faced challenges in minimizing false damage locations.

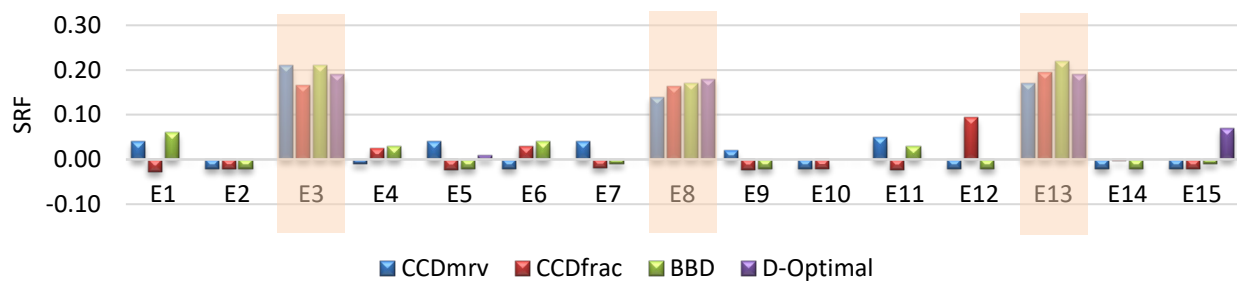


Fig. 6. SRF from CCDmrv, CCDfrac, BBD and D-Optimal for 15 elements

Finer details are achieved with 20 elements, providing a more accurate depiction of stiffness changes due to damage. This results in a higher SRF, around 0.3, reflecting enhanced model resolution. Figure 7 highlights BBD's commendable ability to identify multiple damage locations, especially with lower measurement points. While D-Optimal design accurately identified damage, it exhibited minor false damage location with 20 elements. However, for lower measurement points, it faced challenges in precisely localizing true damage locations.

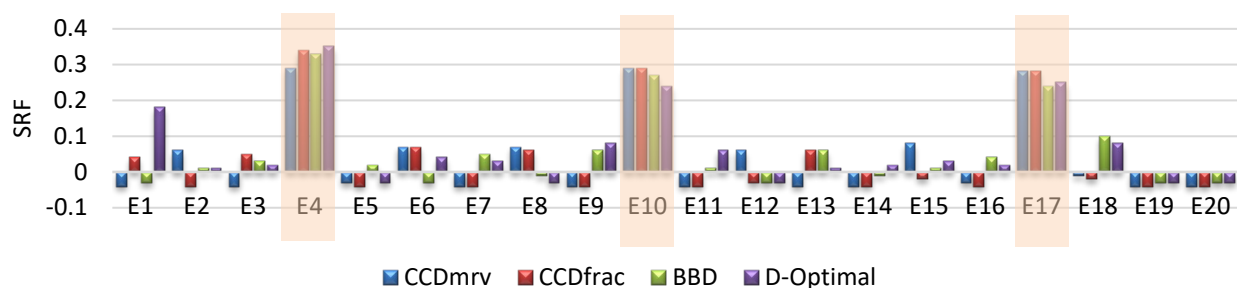


Fig. 7. SRF from CCDmrv, CCDfrac, BBD and D-Optimal for 20 elements

4.2 False Damage Detection

Figure 8 presents a graph depicting the percentage of damage detection error for different DOEs across various measurement points. Generally, a lower error percentage indicates better convergence and optimization performance, while a higher percentage suggests less effective convergence. The convergence graph underscores the importance of selecting the most appropriate measurement points based on the DOE and desired convergence criteria. For instance, while CCDmrv shows relatively consistent performance across measurement points, other DOEs like D-Optimal display more variability, with higher error percentages observed as the number of measurement points increases.

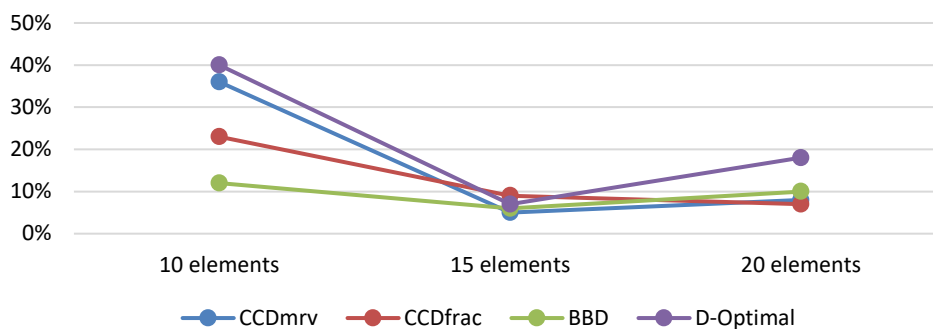


Fig. 8. Damage detection error for various DOEs across measurement points

5. Conclusions

The results of this study provide valuable insights into the performance of different DOE for identifying damage. BBD emerges as particularly effective in detecting multiple damages with fewer measurement points, while CCD excels in accurately identifying damage with minimum false damage location in finer points. However, both CCD and D-Optimal encounter challenges with lower measurement points, struggling to pinpoint true damage locations. These findings highlight how DOE and measurement points interact in damage identification, showing strengths and limitations.

In addition, exploring SRF with different measurement points offers insights into structural damage identification. Variations in SRF values highlight the importance of model accuracy in capturing stiffness changes from damage. Higher measurement points yield refined models and higher SRF values. For instance, SRF around 0.10 with 10 elements gives a general damage idea, while 15 elements yield an SRF around 0.20, offering more precision. SRF around 0.3 with 20 elements captures stiffness reduction well. These results emphasize the balance between computational efficiency and model accuracy. Coarser measurement points might be faster but underestimate damage, while finer measurement points are accurate but computationally demanding. The choice depends on analysis goals and resources.

In conclusion, this study underscores choosing the right measurement points to capture damage response intricacies, enhancing reliability of damage assessment. However, it's important to acknowledge the limitations of the presented technique. While the approach shows promise, it may not be suitable for all scenarios, particularly those with highly complex structures or limited resources for extensive measurements. Future research should address these limitations and explore avenues for further improving the reliability and applicability of the proposed damage identification method.

Acknowledgement

The research was funded by the Ministry of Higher Education (MOHE) under the Fundamental Research Grant Scheme (FRGS), UTM, FRGS/1/2022/TK10/UTM/02/41 and supported by Universiti Teknologi Malaysia (UTM). The first author was funded by the Ministry of Higher Education of Malaysia under Hadiah Latihan Persekutuan (HLP).

References

- [1] Sukri, Nur Raihana, Nurulakmar Abu Husain, Syarifah Zyurina Nordin, and Mohd Shahrir Mohd Sani. "Structural Damage Identification Using Model Updating Approach: A Review." *Journal of Advanced Research in Applied Mechanics* 84, no. 1 (2021): 1-12.
- [2] Alshalal, Iqbal, Muslim Ali, J. H. Mohmmed, and Arshad Abdula Rashed. "Frequency response function curvature technique to detect damage for simply supported beam under harmonic excitation." In *AIP Conference Proceedings*, vol. 2386, no. 1. AIP Publishing, 2022. <https://doi.org/10.1063/5.0066901>
- [3] Sampaio, R. P. C., N. M. M. Maia, and J. M. M. Silva. "Damage detection using the frequency-response-function curvature method." *Journal of sound and vibration* 226, no. 5 (1999): 1029-1042. <https://doi.org/10.1006/jsvi.1999.2340>
- [4] Nayyar, Ayisha, Ummul Baneen, Syed Abbas Zilqurnain Naqvi, and Muhammad Ahsan. "Detection and localization of multiple small damages in beam." *Advances in Mechanical Engineering* 13, no. 1 (2021): 1687814020987329. <https://doi.org/10.1177/1687814020987329>
- [5] Porcu, M. C., D. M. Patteri, S. Melis, and F. Aymerich. "Effectiveness of the FRF curvature technique for structural health monitoring." *Construction and Building Materials* 226 (2019): 173-187. <https://doi.org/10.1016/j.conbuildmat.2019.07.123>
- [6] Box GEP, Wilson KB. "On the Experimental Attainment of Optimum Conditions." *J. Roy. Statist. Soc. Ser. B* 13 (1951). <https://doi.org/10.1111/j.2517-6161.1951.tb00067.x>
- [7] Marwala, Tshilidzi. *Finite element model updating using computational intelligence techniques: applications to structural dynamics*. Springer Science & Business Media, 2010. <https://doi.org/10.1007/978-1-84996-323-7>
- [8] Umar, Sarehati, Norhisham Bakhary, and A. R. Z. Abidin. "Response surface methodology for damage detection using frequency and mode shape." *Measurement* 115 (2018): 258-268. <https://doi.org/10.1016/j.measurement.2017.10.047>
- [9] Yang, Xiuming, Xinglin Guo, Huajiang Ouyang, and Dongsheng Li. "A Kriging model based finite element model updating method for damage detection." *Applied Sciences* 7, no. 10 (2017): 1039. <https://doi.org/10.3390/app7101039>
- [10] Friswell, Michael I. "Damage identification using inverse methods." *Philosophical Transactions of the Royal Society A: Mathematical, Physical and Engineering Sciences* 365, no. 1851 (2007): 393-410. <https://doi.org/10.1098/rsta.2006.1930>
- [11] Hou, Rongrong, and Yong Xia. "Review on the new development of vibration-based damage identification for civil engineering structures: 2010–2019." *Journal of Sound and Vibration* 491 (2021): 115741. <https://doi.org/10.1016/j.jsv.2020.115741>
- [12] Yan, Y. J., Li Cheng, Z. Y. Wu, and L. H. Yam. "Development in vibration-based structural damage detection technique." *Mechanical systems and signal processing* 21, no. 5 (2007): 2198-2211. <https://doi.org/10.1016/j.ymsp.2006.10.002>
- [13] Kong, Xuan, Chun-Sheng Cai, and Jiexuan Hu. "The state-of-the-art on framework of vibration-based structural damage identification for decision making." *Applied Sciences* 7, no. 5 (2017): 497. <https://doi.org/10.3390/app7050497>
- [14] Salawu, Olusegun S. "Detection of structural damage through changes in frequency: a review." *Engineering structures* 19, no. 9 (1997): 718-723. [https://doi.org/10.1016/S0141-0296\(96\)00149-6](https://doi.org/10.1016/S0141-0296(96)00149-6)
- [15] Kumar, K. Arun, and D. Mallikarjuna Reddy. "Application of frequency response curvature method for damage detection in beam and plate like structures." In *IOP conference series: materials science and engineering*, vol. 149, no. 1, p. 012160. IOP Publishing, 2016. <https://doi.org/10.1088/1757-899X/149/1/012160>
- [16] Alpaslan, Emre, and Zeki Karaca. "Response surface-based model updating to detect damage on reduced-scale masonry arch bridge." *Structural Engineering and Mechanics, An Int'l Journal* 79, no. 1 (2021): 9-22.
- [17] Kumar, Anjneya, and Koushik Roy. "Response surface-based structural damage identification using dynamic responses." *Struct. J.* 29 (2020): 1047-1058. <https://doi.org/10.1016/j.istruc.2020.11.033>

- [18] Cundy, A. L., Francois M. Hemez, Daniel J. Inman, and Gyuhae Park. "Use of response surface metamodels for damage identification of a simple nonlinear system." *Key Engineering Materials* 245 (2003): 167-174. <https://doi.org/10.2172/812182>
- [19] Rutherford, A. C., Daniel J. Inman, G. Park, and F. M. Hemez. "Use of response surface metamodels for identification of stiffness and damping coefficients in a simple dynamic system." *Shock and Vibration* 12, no. 5 (2005): 317-331. <https://doi.org/10.1155/2005/484283>
- [20] Mondal, Subhajit, Bidyut Mondal, Anila Bhutia, and Sushanta Chakraborty. "Damage detection in beams using frequency response function curvatures near resonating frequencies." In *Advances in Structural Engineering: Dynamics, Volume Two*, pp. 1563-1573. Springer India, 2015. https://doi.org/10.1007/978-81-322-2193-7_119
- [21] Ren, Wei-Xin, and Hua-Bing Chen. "Finite element model updating in structural dynamics by using the response surface method." *Engineering structures* 32, no. 8 (2010): 2455-2465. <https://doi.org/10.1016/j.engstruct.2010.04.019>
- [22] Fang, Sheng-En, and Ricardo Perera. "A response surface methodology based damage identification technique." *Smart Materials and Structures* 18, no. 6 (2009): 065009. <https://doi.org/10.1088/0964-1726/18/6/065009>
- [23] Myers, Raymond H. "Response surface methodology—current status and future directions." *Journal of quality technology* 31, no. 1 (1999): 30-44. <https://doi.org/10.1080/00224065.1999.11979891>